



Published in final edited form as:

J Phys Chem B. 2019 March 07; 123(9): 2114–2122. doi:10.1021/acs.jpcc.8b12157.

Heterogeneous and Highly Dynamic Interface in Plastocyanin –Cytochrome *f* Complex Revealed by Site-Specific 2D-IR Spectroscopy

Sashary Ramos[†], Amanda L. Le Sueur[†], Rachel E. Horness[‡], Jonathan T. Specker[§],
Jessica A. Collins, Katherine E. Thibodeau, and Megan C. Thielges^{*}

Indiana University, Department of Chemistry, Bloomington, Indiana 47405, United States

Abstract

Transient protein complexes are crucial for sustaining dynamic cellular processes. The complexes of electron-transfer proteins are a notable example, such as those formed by plastocyanin (Pc) and cytochrome *f* (cyt *f*) in the photosynthetic apparatus. The dynamic and heterogeneous nature of these complexes, however, makes their study challenging. To better elucidate the complex of *Nostoc* Pc and cyt *f*, 2D-IR spectroscopy coupled to site-specific labeling with cyanophenylalanine infrared (IR) probes was employed to characterize how the local environments at sites along the surface of Pc were impacted by cyt *f* binding. The results indicate that Pc most substantially engages with cyt *f* via the hydrophobic patch around the copper redox site. Complexation with cyt *f* led to an increase in inhomogeneous broadening of the probe absorptions, reflective of increased heterogeneity of interactions with their environment. Notably, most of the underlying states interconverted very rapidly (1 to 2 ps), suggesting a complex with a highly mobile interface. The data support a model of the complex consisting of a large population of an encounter complex.

Additionally, the study demonstrates the application of 2D-IR spectroscopy with site-specifically introduced probes to reveal new quantitative insight about dynamic biochemical systems.

Graphical Abstract

^{*}Corresponding Author thielges@indiana.edu.

[‡]R.E.H.: Rose-Hulman Institute of Technology, Department of Chemistry, Terre Haute, IN 47803.

[§]J.T.S.: University of Florida, Department of Chemistry, Gainesville, FL 32611.

[†]S.R. and A.L.L.S. contributed equally.

Author contributions

The manuscript was written through contributions of all authors. All authors have given approval to the final version of the manuscript.

Notes

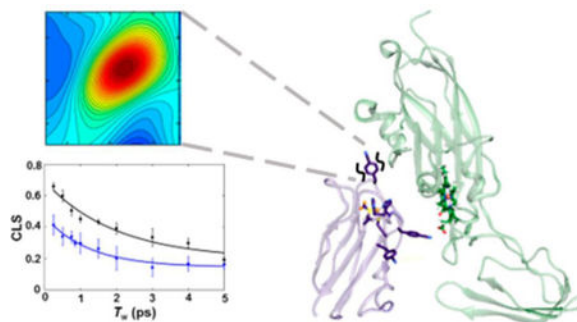
The authors declare no competing financial interest.

ASSOCIATED CONTENT

Supporting Information

The Supporting Information is available free of charge on the ACS Publications website at DOI: [10.1021/acs.jpcc.8b12157](https://doi.org/10.1021/acs.jpcc.8b12157).

Figures S1–S6. Experimental details of protein expression, spectroscopic measurements, and analysis; mass, circular dichroism, and UV-visible spectra of Pc variants (PDF)



INTRODUCTION

Protein–protein interactions underlie all cellular processes. Some proteins form tightly associated, well-defined complexes, well captured by crystal structures. However, many others must interact with their partners with lower affinity to form transient complexes so as to ensure rapid turnover in their cellular function.^{1,2} Dynamic complexes, for example, are formed by recognition domains for fast response in signaling networks and by electron-transfer (ET) proteins for mediating efficient electron transport in diverse processes, including photosynthesis and respiration.^{3–5} The dynamic nature makes these protein complexes more challenging to investigate and describe, hindering the development of a complete mechanistic understanding of their function.

A dynamic complex of central importance in photosynthesis forms between ET partners plastocyanin (Pc) and cytochrome *f* (cyt *f*).^{6,7} Pc is a small, soluble protein with a type-I copper site that functions as an electron shuttle from the cytochrome *b₆ f* complex to photosystem I (Figure 1). Cyt *f* has a short C-terminal tail that anchors it to the thylakoid membrane, but the majority is a soluble protein that consists of an elongated structure of two domains, the larger of which contains a heme cofactor. Pc and cyt *f* must sufficiently engage to bring the redox centers in proximity to ensure the efficient transfer of electrons yet transiently to maintain the redox flux in photosynthesis. The interactions formed in such protein–protein complexes must be specific but highly dynamic.

In general, any mechanism of protein molecular recognition involves the initial approach of proteins to form an encounter complex, a loosely associated state that potentially includes a range of protein–protein orientations.⁹ For high-affinity complexes, this step is followed by the evolution of the ensemble into a single, well-defined complex. However, transient protein complexes, such as those formed by Pc and cyt *f*, are thought to exist as an ensemble that can contain a large population of a loosely bound state akin to the encounter complex.^{4,10,11} This population is in rapid exchange with a more well-defined state that is presumably more optimal for ET.

Whereas this model generally describes the recognition of Pc and cyt *f*, the exact nature of their complexes and critical molecular interactions remains under question and, furthermore, varies among species.^{4,7,12–14} The complexes can be stabilized by two regions of the proteins (Figure 1). A set of nonpolar residues surrounds the redox cofactors of both proteins

creating “hydrophobic patches”. The proteins also can contain “electrostatic patches” formed by clusters of charged residues. How these regions are variably involved in forming the complexes of Pc and cyt *f* homologues has been under investigation, primarily through the analysis of ET kinetics and mapping of the interactions by nuclear magnetic resonance (NMR) spectroscopy.^{13,15–21} Electrostatic interactions contribute to the binding of plant, algal, and some cyanobacterial proteins; however, the charge complementarity of Pc and cyt *f* is species-dependent. For example, Pc and cyt *f* of *Nostoc* sp. PCC7119 cyanobacteria are positively and negatively charged, respectively, whereas the plant proteins display the opposite charge complementarity.^{15,20,22} For these homologues, the models of the complexes derived from NMR spectroscopy, exhibit extensive contact involving both the hydrophobic patch at the “head” and the electrostatic patch at the “side” of Pc.^{13,15,23,24} At another extreme, the proteins from some cyanobacteria, such as *Phormidium laminosum*, lack significant electrostatic patches, and the binding is exclusively mediated via hydrophobic interactions in a head-on manner.¹⁶

Along with the disparate stabilizing interactions and engagement, homologous complexes of Pc and cyt *f* also show diversity in the nature of their bound states, the extent the ensembles populate encounter or well-defined complexes. Whereas our understanding of the ensembles is limited, NMR paramagnetic relaxation (PRE) spectroscopy in combination with ensemble modeling has provided insight into their heterogeneous and varying composition.^{13,23–26} A large population of encounter complex appears to be populated by the cyanobacterial homologues of *P. laminosum* and *Prochlorothrix hollandica*, which lack stabilizing electrostatic interactions, compared with the complexes of proteins with electrostatic complementarity, such as the plant and algal proteins.^{16,27} However, *Nostoc* Pc and cyt *f* have electrostatic complementarity but nevertheless appear to form a highly dynamic complex consisting of a large population of encounter state.²⁴ Unfortunately, the available experimental data are insufficient to completely define the complex. Not only is the complex a heterogeneous ensemble but also a challenge arises from the fast time scales of interconversion between the free state and the encounter complex and between the encounter complex and the well-defined state, as both processes are rapid on the NMR time scale. The investigation of these dynamic complexes would be facilitated by complement with experimental approaches with faster inherent time scales.

Infrared spectroscopy has emerged as a powerful tool for the study of proteins and their dynamics due to its potential for excellent spatial and temporal resolution. To avoid the problem of spectral congestion, the approach may be combined with the site-specific incorporation of vibrational groups that have infrared (IR) absorptions in a transparent frequency window of a protein IR spectrum, thereby enabling the characterization of specific local environments and dynamics in proteins.^{28–30} The frequency, line width, and number of unique bands of the IR probes report on the nature, heterogeneity, and number, respectively, of the environments surrounding the probe. Two-dimensional (2D) IR spectroscopy enables the measurement of the inhomogeneity of the probe frequencies, which affords a more rigorous measure of local heterogeneity.^{31,32} Moreover, time-dependent 2D-IR experiments can follow in real time the dynamics among the frequency distribution (spectral diffusion), providing a direct measure of the dynamics of the interaction of the probe with its environment.^{33–39}

We applied 1D and 2D spectroscopy in combination with site-selective labeling with IR probes toward better understanding the complexes formed between Pc and cyt *f* from *Nostoc* cyanobacteria. Nitrile IR probes were introduced by the selective incorporation of cyanophenylalanine (*CNF*) via amber suppression at three distinct locations in Pc (Figure 1). One probe was placed at the head of Pc in the hydrophobic patch surrounding the copper redox site (*CNF36*), another was placed at the side of Pc in the electrostatic patch (*CNF88*), and the last was placed in a loop between two of the copper ligands (Cys89 and His91) located at the border of the hydrophobic and electrostatic patches (*CNF90*). The IR spectra of the *CNF* probes uncovered variation in the local environments along the surface of Pc and in the impact from binding with cyt *f*. Additionally, 2D-IR spectroscopy indicated a substantial increase in the inhomogeneity of the environments of the probes in the complex, reflective of heterogeneous interactions with the surface of cyt *f*. Interestingly, the majority of the states in the bound complex nonetheless interconverted on very rapid (1 to 2 ps) time scales, providing evidence of a large population of the encounter complex with a highly mobile protein–protein interface.

MATERIALS AND METHODS

Preparation and Characterization of cyt *f* and Pc Variants.

cyt *f* and wild-type Pc were expressed and purified as previously described with some modifications.⁴⁰ As in the previous biophysical studies of cyt *f*,^{20,21,41} the truncated construct lacking the transmembrane helix was used for its higher solubility. *CNF* incorporation at three distinct locations of Pc was achieved in vivo using the amber codon suppressor method.⁴² The proteins were characterized by mass spectrometry, circular dichroism (CD) spectroscopy, and UV–visible spectroscopy. Binding constants (K_D) for each Pc variant to cyt *f* were determined via a fluorescence assay. Details regarding protein preparation and characterization are provided in the Supporting Information.

Sample Preparation for 1D -and 2D-IR Spectroscopy.

Purified Pc variants and cyt *f* were exchanged into 1 mM sodium phosphate, pH 6.8. For FT-IR spectroscopy, samples of the free Pc were prepared at 2 mM, whereas samples of the cyt *f* complex were prepared at concentrations expected to result in >92% bound Pc for all variants on the basis of the measured K_D values. FT-IR samples were sealed between two CaF₂ windows separated by a 38.1 μ m spacer. For 2D-IR spectroscopy, samples of free Pc were prepared at concentrations of 3.2 to 4.8 mM and sealed between two CaF₂ windows separated by a 127 or 76 μ m spacer. Samples of the Pc and cyt *f* complex for 2D-IR spectroscopy were prepared with cyt *f* at concentrations expected to result in ~94% bound Pc for all variants on the basis of the measured K_D values. All 2D-IR samples of the Pc-cyt *f* complex were sealed between two CaF₂ windows separated by a 76 μ m spacer. More details regarding sample preparation can be found in the Supporting Information.

1D- and 2D-IR Spectroscopy.

FT-IR spectra were collected on an Agilent Cary 670 FT-IR spectrometer using a liquid-N₂-cooled mercury–cadmium–telluride (MCT) detector. Details regarding spectral acquisition and processing are provided in the Supporting Information. A residual slowly varying

baseline in the absorption spectra was removed by fitting a polynomial to a spectral region excluding the CN absorption bands (MATLAB 7.8.0). The absorption bands of the baseline-corrected spectra were then fit to Gaussian functions to determine the center frequencies and line widths (Figure 2, Table 1).

2D-IR spectroscopy was conducted as previously described.^{43–45} In brief, a Ti:sapphire oscillator/regenerative amplifier (Spectra Physics) producing ~ 75 fs pulses centered at 800 nm with 1 kHz repetition rate was used to pump a home-built optical parametric amplifier to generate the ~ 170 fs pulses centered at 2225 cm^{-1} (80 cm^{-1} fwhm) used in the experiments. 2D-IR experiments were performed in the conventional BOXCAR geometry, and 2D-IR spectra were generated as previously reported. Additional experimental details are available in the Supporting Information.

2D-IR spectroscopy provides correlation spectra that associate the initial (ω_i) and final (ω_f) frequencies of the *CMF* probes within the ensemble measured with a time separation, the waiting time (T_w) (Figure 3). At the shortest T_w values, the 2D bands appear elongated along the diagonal, reflecting the high correlation between the frequency axes because the system has not had time to significantly evolve. With increasing T_w , the bands become less elongated as amplitude grows in off the diagonal, reflecting that part of the distribution of underlying microstates experienced by the *CMF* has interconverted during T_w . The evolution of the 2D lineshapes of the *CMF* probe with increasing T_w follows its spectral dynamics (spectral diffusion), which can be described by frequency–frequency correlation functions (FFCFs). The FFCF was extracted from the 2D data via center line slope (CLS) analysis of the 2D lineshapes. The CLS decay curves (Figure 4) approximate the normalized inhomogeneous contribution to the FFCF; combined fitting of the CLS decay and the linear spectra yield the full FFCFs.⁴⁶

The FFCFs were analyzed according to the Kubo model using the equation⁴⁷

$$\text{FFCF} = \frac{\delta(t)}{T_2} + \Delta_1^2 e^{-t/\tau_1} + \Delta_S^2$$

The latter two terms describe the dynamics among the inhomogeneous distribution of frequencies underlying the absorption bands. The inhomogeneous dynamics are separated into two time scales, where Δ_1^2 is the variance in frequencies sampled on the faster time scale, τ_1 , and the static term, Δ_S^2 , is the variance in frequencies sampled more slowly than the experimental time window. The first term, $\delta(t)/T_2$, where $1/T_2 = (1/T_2^*) + (1/2T_1)$, accounts for the homogeneous contribution to the FFCF. T_1 is the vibrational lifetime, which was previously measured to be 4.2 ps.⁴⁵ The pure dephasing time, $T_2^* = (\Delta^2 \tau)^{-1}$, describes very fast fluctuations that are in the motionally narrowed limit on the IR time scale, where the frequency amplitude and time scale cannot be separated ($\tau \ll 1$). The homogeneous dynamics lead to a Lorentzian contribution to the line shape, $\Gamma^* = 1/\pi T_2^*$.

RESULTS

Preparation and Characterization of CNF-Labeled Pc.

To introduce frequency-resolved IR probes in Pc, CNF was selectively incorporated via amber suppression.⁴² The sites of labeling were selected to probe *Nostoc* Pc at two regions, the hydrophobic and electrostatic patches, which prior studies implicate in the binding of Pc to cyt *f*.^{20,23} A native tyrosine (Tyr88) is located near the electrostatic patch next to Arg93, a residue previously shown to facilitate ET with cyt *f* via electrostatic interactions.¹⁸ The substitution of CNF88 for a tyrosine was expected to be minimally perturbative, and it enabled the investigation of the interaction with cyt *f* along the side of Pc. We then consulted prior studies of homologous sequence analysis to identify nonconserved residues in Pc as candidates for probe placement.⁴⁸ The substitution of Val36 with CNF36 introduced an IR probe along a series of nonpolar residues surrounding the copper site that form the hydrophobic patch. CNF36 enabled investigation of the interaction with cyt *f* at the head of Pc. Finally, CNF was introduced at Glu90, located at the edge of the head of Pc near the boundary of the hydrophobic and electrostatic patches. We note that this substitution removed a negatively charged residue. Although not desirable, the substitution was anticipated to enhance rather than weaken the electrostatic interaction of the positively charged Pc with the negatively charged cyt *f* of *Nostoc* cyanobacteria, and, as expected, the CNF90 Pc showed higher affinity for cyt *f* (vide infra). Unfortunately, in comparison with our experience with other proteins (e.g., cytochrome P450cam and SH3 domains),^{49,50} we found that Pc was less amenable to labeling with CNF via amber suppression. Constructs were made to incorporate CNF at 10 additional sites in Pc, but initial efforts to screen expression obtained no or misfolded protein, and thus more comprehensive labeling will require additional optimization of expression conditions.

Each Pc variant was characterized for potential perturbation from CNF incorporation. UV–visible CD and absorption spectroscopy confirmed that no perturbation occurred to the secondary structure or copper site (Figures S2 and S3), respectively. The affinity of each protein for cyt *f* was assessed by monitoring the change in fluorescence of cyt *f* upon titration with increasing concentration of Pc (Figure S5). The K_D for binding cyt *f* of $70 \pm 10 \mu\text{M}$ determined for the wild-type Pc was in agreement with previously reported values.^{13,23,25} The K_D of $50 \pm 10 \mu\text{M}$ for binding of CNF36 Pc and cyt *f* was measured to be only slightly smaller than the wild-type, indicating no substantial perturbation to the complex by probe incorporation. In comparison, CNF88 and CNF90 incorporation more significantly increased the affinity for cyt *f* (K_D values of $10 \pm 6 \mu\text{M}$ and $1.2 \pm 1.1 \mu\text{M}$, respectively). The higher affinity resulting from the replacement of the negatively charged glutamate residue by CNF90 is consistent with prior mutagenesis studies that implicated electrostatic interactions in stabilizing *Nostoc* Pc-cyt *f* binding.^{18,20} In contrast, the increased affinity of CNF88 for Pc was more surprising, as mutation of this residue to alanine or phenylalanine has no effect on ET kinetics.¹⁸ Although the potential influence of the CNF probes on the complex should be kept in mind, we nonetheless could use the determined K_D values to prepare samples at Pc and cyt *f* concentrations expected to ensure a ~94% shift of the Pc population to the bound complex.

FT-IR Spectroscopy.

FT-IR spectroscopy was applied first to each *CNF* in the free protein to investigate the variation in the environments along the surface of Pc. For all proteins, the IR spectra showed absorption bands for the CN stretch with center frequencies from 2235.2 to 2238.4 cm^{-1} (Figure 2, Table 1), similar to that of free amino acid in solution (2236.7 cm^{-1}). The frequency of a CN probe is sensitive to both long-range electrostatic interactions and short-range interactions such as hydrogen bonding (H bonding) and repulsion due to close packing.^{51–54} The relatively high frequencies observed for the *CNF* in the Pc and aqueous solution are consistent with a polar environment and participation in H bonding, as expected for solvent-exposed residues along the protein surface. Although the frequencies of all were generally high, they varied substantially among the sites and in a manner reflective of their local environment. Of the probes, *CNF36* within the hydrophobic patch showed the lowest frequency, indicative of a relatively nonpolar environment with reduced H bonding. At the other extreme, *CNF88* within the electrostatic patch showed the highest frequency, whereas *CNF90* at the junction of the hydrophobic and electrostatic patches showed intermediate frequency. For both *CNF88* and *CNF90*, the frequencies were even higher than those found in aqueous solution, where blue-shifting from H bonding to water is likely as or more extensive, implying that the solvatochromism of the CN also involves substantial contributions from electrostatic or electronic repulsion from their local environments.

To investigate the involvement of each *CNF* in binding to cyt *f*, the Pc variants were next characterized in the complex. For all sites, the CN absorption shifted to lower frequency upon binding cyt *f*, indicative of a less polar environment or reduction in H bonding. The degree of the change, however, differed among them. The absorption of *CNF36* was most highly impacted (shifting by 3 cm^{-1}), indicating substantial changes to the environment at the hydrophobic patch of Pc. In comparison, the absorption of *CNF90* was only moderately affected (1 cm^{-1}), and that of *CNF88* was even less so (0.6 cm^{-1}). In addition to shifting the CN frequency, binding cyt *f* led to broader absorption line widths for all sites. The line-width broadening is consistent with greater heterogeneity in the environment experienced by a CN probe; however, the inhomogeneous line width that reflects the heterogeneous frequency distribution is convoluted with homogeneous line-broadening mechanisms in the linear IR spectra. 2D-IR spectroscopy was employed to better elucidate the spectral broadening as well as measure the dynamics among the inhomogeneous distribution.

2D-IR Spectroscopy.

Time-dependent 2D-IR spectra of the free Pc and complex with cyt *f* (Figure 3) were acquired and analyzed to obtain FFCFs of each *CNF* (Table 1, Figure 4). The FFCFs provide richer insight into the contributions to the line broadening of the CN absorptions. Specifically, our analysis deconvoluted the contribution from motions that are very fast on the IR time scale (homogeneous broadening) and those that result from the distribution of microenvironments experienced by the CN probe in the sample ensemble (inhomogeneous broadening). In addition, the FFCFs provided the time scales over which the inhomogeneous distribution of states interconverts and thus information about the dynamics of the interaction of the CN with its environment.

The FFCFs measured for the Pc variants captured dynamics on three distinct time scales: very fast homogeneous dynamics (Γ^*), inhomogeneous dynamics on the 1 to 2 ps time scale (τ_1), and inhomogeneous dynamics slower than the experimental time window (τ_2) (Table 1). Although the FFCFs for the Pc variants exhibited similar time scales, they also revealed site-specific differences both among the free proteins and in the effects of cyt *f* binding. For free Pc, the FFCF of *CNF88* was essentially the same as that for an aqueous solution of the amino acid. In comparison, the FFCF of *CNF90* was distinct in showing greater homogeneous broadening and a smaller inhomogeneous contribution associated with the 1.2 ps dynamics (τ_1). This observation indicates a relatively high contribution to the line broadening from states with interconversion in the fast as opposed to slow exchange regime of IR spectroscopy and is suggestive of overall faster dynamics on the few picoseconds and shorter time scale. Finally, the FFCF of *CNF36* showed the largest inhomogeneous broadening, associated with both rapidly and slowly interconverting states, indicative of overall greater heterogeneity.

To next assess the involvement of each site in binding to cyt *f*, the FFCFs at each *CNF* for the complexes with cyt *f* were compared with those for the free proteins (Table 1). *CNF36* and *CNF90* were most highly impacted by cyt *f* binding. For both probes, the value of the CLS derived from the 2D spectrum at the shortest T_w became much larger in the complex (Figure 4). This result reflects a decrease in homogeneous broadening and a large increase in inhomogeneous broadening, which indicates a large increase in the heterogeneity of the environment of both *CNF36* and *CNF90* when in the complex. Although the increased inhomogeneity was sampled on both fast and slow time scales, a larger contribution was associated with rapidly interconverting states (τ_1) (Figure 5). In comparison with *CNF36* and *CNF90*, the FFCF for *CNF88* was less sensitive to cyt *f* binding but also showed a small increase in inhomogeneity, reflecting the greater heterogeneity of interactions with its environment. For *CNF88*, unlike the other two sites, cyt *f* binding resulted in an increase in homogeneous broadening and a faster time scale of inhomogeneous dynamics, suggestive of overall faster dynamics on the few picoseconds and shorter time scale. These observations could arise from perturbation to the surrounding water dynamics or proximity of fluctuating charged residues of cyt *f*.

DISCUSSION

FT-IR and 2D-IR spectroscopy of the site-specifically incorporated *CNF* probes enabled the characterization of the distinct local environments along the surface of Pc. The average absorption frequencies of the probes reflected the polarity and H-bonding capability of their surrounding environments in the hydrophobic or electrostatic regions of the Pc surface. The inhomogeneity and dynamics measured by 2D-IR spectroscopy also revealed differences in the heterogeneity and motion. *CNF36* showed the largest heterogeneity, which reasonably could result from the probe's significant exposure to both polar solvent and nearby nonpolar residues in the environment of the hydrophobic patch. In contrast, *CNF90* showed overall faster dynamics on the few picoseconds and shorter time scale. Such fast time scales are suggestive of water or small-scale side-chain dynamics uniquely sensed at *CNF90*,^{55,56} which could arise from the particular environment near the junction of the hydrophobic and electrostatic surfaces. *CNF88* showed heterogeneity and dynamics similar to the amino acid

in aqueous solution, indicating that its environment in the electrostatic patch is most like that of mobile water. Altogether, the linear and 2D data illuminate the complex, heterogeneous surface of Pc.

Furthermore, the linear and 2D-IR data reveal the sitespecific sensitivity of the probes to association with cyt *f* that provides evidence of variable involvement along the surface of Pc in the complex. The induced changes in the average absorption frequency and frequency inhomogeneity were larger for *CMF36* and *CMF90* in comparison with *CMF88*, implying that complexation with cyt *f* more strongly impacts their locations. These results suggest that Pc engages with cyt *f* more substantially via the hydrophobic than the electrostatic patch and support a model of the complex in which the head of Pc more appreciably contacts cyt *f*. In such a complex, longer-range electrostatic forces involving the electrostatic side of Pc could stabilize the complex with cyt *f* while not necessarily entailing significant perturbation to the Pc surface. This interpretation is consistent with our understanding of the *Nostoc* protein complex derived from NMR spectroscopy.^{21,23} Both *CMF36* and *CMF90* are among a series of residues along the head of Pc with amide backbone resonances that show the large chemical shift perturbation and pseudocontact shifts (PCSs) from interaction with the paramagnetic heme or spin labels placed on cyt *f*.^{21,23} In contrast, the backbone NMR resonances and the present IR data for *CMF88* are less affected by cyt *f* binding. In addition, previous studies found that the mutation of Y88 to alanine or phenylalanine does not affect ET kinetics, but substitution of surrounding residues to remove the positive charge does,¹⁸ supporting the involvement of the region primarily via longer-range electrostatic interactions.

The increase in inhomogeneity for all probes in the complex with cyt *f* indicates that the surface of Pc experiences greater heterogeneity upon interaction with its binding partner. Surprisingly, the increased inhomogeneity was mostly associated with states that interconvert on the 1 to 2 ps time scale (τ_1), not with states that interconvert slowly (τ_2) (Figure 5), as anticipated for strong interactions formed within a tightly engaged surface. This behavior is apparent qualitatively from an inspection of the CLS curves for *CMF36* and *CMF90* shown in Figure 4. The values of the CLS for these probes at the earliest T_w (0.25 ps) increased dramatically in the complexes, indicative of greater inhomogeneity, but the CLS curves still decayed rapidly, showing that the heterogeneity is rapidly sampled. At the longest T_w in the experimental time window, the CLS values were only slightly larger for the complexes than the free proteins, implying similar inhomogeneity from slowly interconverting states. These results are unusual when compared with our and others' previous 2D-IR studies of *CMF* and other IR probes incorporated into proteins, which typically find large effects to the slowest or static component of the FFCFs arising from sensitivity to the slow motions in proteins.³³⁻³⁹ For example, *CMF* probes placed within the HP35 peptide report a large increase in inhomogeneity from slowly interconverting states when the peptide folds into a domain.³³ Similarly, site-specific *CMF* probes placed along the surface of a SRC-homology-3 domain to characterize its association with a peptide ligand showed inhomogeneity from slowly interconverting states the most substantially impacted.³⁴ Studies that employed IR probes other than *CMF* report similar findings. For example, azidohomoalanine probes incorporated along a peptide ligand of a PDZ domain show increased inhomogeneity associated with slow dynamics induced by protein-ligand

association.³⁵ Upon the incorporation into lysozyme, metal carbonyl side-chain probes show a large increase in static inhomogeneity attributed to slower protein motion,³⁶ which further increases upon the addition of protein-crowding agents.³⁷ Similarly, substantial variation in inhomogeneity with slow dynamics is observed for enzyme complexes using ligand-based IR probes, such as the azide ion and azido-functionalized cofactor analogs.^{38,39} In contrast, the increase in inhomogeneity found for the *CNF* probes of Pc in the complex with cyt *f* was mostly associated with fast dynamics. This implies that in the complex the probes experience an increase in heterogeneity of states that interconverts rapidly. This finding seems inconsistent with a bound complex involving a tightly engaged protein–protein interface but rather supports a model consisting of a substantial population in which the surface retains a layer of mobile water or the side chains remain highly mobile.

A possible explanation for the rapid dynamics found in the bound complex is that the ensemble consists of a large population of a loosely associated state, an encounter complex, as has been proposed from previous NMR studies.^{13,24} Ensemble modeling of the *Nostoc* Pc-cyt *f* complex with constraints from NMR PRE measurements was not consistent with the population of a single, well-defined state. In addition, similar maps of PCSs were obtained for Pc when spin labels were placed at disparate sites of cyt *f*, indicating diffuse areas of contact. However, our understanding of the complex remains limited. The heterogeneous ensemble of the encounter complex involves many states that rapidly interconvert, and not only does such complexity present an inherent challenge for investigation but also NMR spectroscopy provides information only about the population-weighted average of such dynamic states. In comparison, the well-defined state, the encounter complex, and the states that make up the encounter complex are expected to interconvert slowly on the IR time scale (ps), such that they lead to frequency inhomogeneity, as found for the *CNF* probes in Pc. Whereas the increase in inhomogeneity measured upon binding to cyt *f* was variable among the *CNF* probes, it is notable that for all probes the magnitude of the change associated with rapid dynamics was about three times greater than that associated with slow dynamics (Figure 5). Although the dynamics at each probe might arise from motions of the interactions particular to its environment, the equivalence of the relative increases in the inhomogeneous components for all of the probes suggests that they might inform generally about the populations of states adopted by the bound complex. As an exercise to gain insight into the composition of the ensemble, we assume that the surface remains highly mobile in an encounter complex, whereas it becomes restricted in a well-defined state. We then consider the total increase in frequency inhomogeneity to reflect the total increase in heterogeneity upon complexation and attribute the part of the inhomogeneity with rapid dynamics to the population of the encounter state and that with slow dynamics to a well-defined, specific state. Such analysis yields a rough estimate of 75% of the bound complex populating the encounter state. This estimate is likely to be a lower limit, as the encounter and well-defined states themselves are also expected to lead to inhomogeneity that interconverts very slowly relative to the 2D-IR time window.

Despite the simplistic analysis, the 2D-IR data support the notion that the population of the encounter complex for *Nostoc* Pc and cyt *f* is very large. Other ET partners similarly show a large population of the encounter complex. For example, an exclusive population of an encounter complex is observed for some ET proteins, such as for adrenodoxin and

cytochrome P450 and for myoglobin and cytochrome *b*₅.^{57,58} Our previous study of cytochrome P450cam and putidaredoxin measured a state with 25% population that we interpreted as an encounter complex.⁵⁹ An estimated 30% population of the complex of cytochrome *c* and cytochrome *c* peroxidase is attributed to the encounter complex and as much as 80% population for mutated proteins.^{60,61} NMR studies indicate that the Pc/cyt *f* complex of *P. laminosum* is even more dynamic than that formed by the *Nostoc* proteins, which is suggestive of an even higher population of encounter complex.^{13,16} The loosely engaged states historically were thought to be stabilized by electrostatic interactions,^{4,9} however, the *P. laminosum* proteins lack charge complementarity. In addition, more recent NMR and modeling studies of the *Nostoc* homologues have concluded that consideration of electrostatic interactions is not sufficient to describe the encounter complex.^{21,24} Our observation that the probes at the hydrophobic head of *Nostoc* Pc were more impacted by complexation but nonetheless retained high mobility suggests their involvement in the encounter complex through diffuse interactions.

CONCLUSIONS

The application of 2D-IR spectroscopy with the selectively incorporated probes provided insight into the nature of the complex of *Nostoc* Pc and cyt *f*. Although all sites of Pc appear involved to some extent in cyt *f* binding, the IR spectral data indicate that the hydrophobic region at the head of Pc more substantially engages cyt *f* than the electrostatic patch. Significantly, 2D-IR spectroscopy enabled the rigorous measurement of a large increase in frequency heterogeneity with rapid dynamics in the complex. These observations provide support for the substantial population of a state in which the protein surface remains highly mobile. We attribute this state to a loosely associated encounter complex and conclude that it makes up a major population for the complex of *Nostoc* Pc and cyt *f*. Such a population would facilitate rapid turnover in the ET reactions required for photosynthesis. As for Pc and cyt *f*, ensembles with a high population of dynamic encounter states are likely to facilitate transient interactions in many other cellular processes. This study demonstrates the potential of site-specific 2D-IR spectroscopy with IR probes as an approach to gain new insight into systems with such rapid dynamics.

Supplementary Material

Refer to Web version on PubMed Central for supplementary material.

ACKNOWLEDGMENTS

We thank Indiana University and the Department of Energy (Early Career Award, DOE/DE-FOA-0000751) for funding. S.R. and R.E.H. thank the Indiana University Chemical and Quantitative Biology Training Grant (T32 GM109825) for partial support.

Biography



Megan Thielges received her Ph.D. in biophysics at The Scripps Research Institute (La Jolla, CA) in 2009 and completed postdoctoral studies in multidimensional IR spectroscopy at Stanford University. In 2012, she joined the faculty at Indiana University and became an associate professor in 2018. Her primary research interests center around elucidating the conformations and dynamics of proteins and understanding how they are involved in function. In support of these goals, her research program aims to advance experimental methods of site-specific linear and multidimensional infrared spectroscopy for characterizing protein dynamics with high spatial and temporal detail.

ABBREVIATIONS

Pc	plastocyanin
Cyt <i>f</i>	cytochrome <i>f</i>
ET	electron transfer
CLS	center line slope
FFCF	frequency–frequency correlation function

REFERENCES

- (1). Nooren IMA; Thornton JM Diversity of Protein-Protein Interactions. *EMBO J* 2003, 22, 3486–3492. [PubMed: 12853464]
- (2). Perkins JR; Diboun I; Dessailly BH; Lees JG; Orengo C Transient Protein-Protein Interactions: Structural, Functional, and Network Properties. *Structure* 2010, 18, 1233–1243. [PubMed: 20947012]
- (3). Stein A; Pache RA; Bernado P; Pons M; Aloy P Dynamic Interactions of Proteins in Complex Networks: A More Structured View. *FEBS J* 2009, 276, 5390–5405. [PubMed: 19712106]
- (4). Ubbink M The Courtship of Proteins: Understanding the Encounter Complex. *FEBS Lett* 2009, 583, 1060–1066. [PubMed: 19275897]
- (5). Acuner Ozbabacan SE; Engin HB; Gursoy A; Keskin O Transient Protein-Protein Interactions. *Protein Eng., Des. Sel* 2011, 24, 635–648. [PubMed: 21676899]
- (6). Sykes AG Plastocyanin and the Blue Copper Proteins. *Struct. Bonding (Berlin, Ger.)* 1990, 75, 175–224.
- (7). Hope AB Electron Transfers Amongst Cytochrome *f*, Plastocyanin and Photosystem I: Kinetics and Mechanisms. *Biochim. Biophys. Acta, Bioenerg* 2000, 1456, 5–26.
- (8). Pettersen EF; Goddard TD; Huang CC; Couch GS; Greenblatt DM; Meng EC; Ferrin TE UCSF Chimera—A Visualization System For Exploratory Research and Analysis. *J. Comput. Chem* 2004, 25, 1605–1612. [PubMed: 15264254]
- (9). Schreiber G; Haran G; Zhou HX Fundamental Aspects of Protein-Protein Association Kinetics. *Chem. Rev* 2009, 109, 839–860. [PubMed: 19196002]

- Author Manuscript
- Author Manuscript
- Author Manuscript
- Author Manuscript
- (10). McLendon G; Zhang Q; Wallin SA; Miller RM; Billstone V; Spears KG; Hoffman BM Thermodynamic and Kinetic Aspects of Binding and Recognition in the Cytochrome *c*/Cytochrome *c* Peroxidase Complex. *J. Am. Chem. Soc* 1993, 115, 3665–3669.
 - (11). Bendall DS; Schlarb-Ridley BG; Howe CJ Transient Interactions between Soluble Electron Transfer Proteins. The Case of Plastocyanin and Cytochrome *f*. In *Bioenergetic Processes of Cyanobacteria*; Peschek GA, Obinger C, Renger G, Eds.; Springer: Dordrecht, The Netherlands, 2011.
 - (12). Hervas M; Navarro JA; De La Rosa MA Electron Transfer between Membrane Complexes and Soluble Proteins in Photosynthesis. *Acc. Chem. Res* 2003, 36, 798–805. [PubMed: 14567714]
 - (13). Scanu S; Forster J; Finiguerra MG; Shabestari MH; Huber M; Ubbink M The Complex of Cytochrome *f* and Plastocyanin from *Nostoc* sp. PCC 7119 Is Highly Dynamic. *ChemBioChem* 2012, 13, 1312–1318. [PubMed: 22619165]
 - (14). Ubbink M Dynamics in Transient Complexes of Redox Proteins. *Biochem. Soc. Trans* 2012, 40, 415–418. [PubMed: 22435822]
 - (15). Ubbink M; Ejdeback M; Karlsson BG; Bendall DS The Structure of the Complex of Plastocyanin and Cytochrome *f*, Determined by Paramagnetic NMR and Restrained Rigid-Body Molecular Dynamics. *Structure* 1998, 6, 323–335. [PubMed: 9551554]
 - (16). Crowley PB; Otting G; Schlarb-Ridley BG; Canters GW; Ubbink M Hydrophobic Interactions in a Cyanobacterial Plastocyanin-Cytochrome *f* Complex. *J. Am. Chem. Soc* 2001, 123, 10444–10453. [PubMed: 11673974]
 - (17). Schlarb-Ridley BG; Bendall DS; Howe CJ Role of Electrostatics in the Interaction between Cytochrome *f* and Plastocyanin of the Cyanobacterium *Phormidium laminosum*. *Biochemistry* 2002, 41, 3279–3285. [PubMed: 11876635]
 - (18). Albarran C; Navarro JA; Molina-Heredia FP; Murdoch P. d. S.; De la Rosa MA; Hervas M Laser Flash-Induced Kinetic Analysis of Cytochrome *f* Oxidation by Wild-Type and Mutant Plastocyanin from the Cyanobacterium *Nostoc* sp. PCC 7119. *Biochemistry* 2005, 44, 11601–11607. [PubMed: 16114897]
 - (19). Lange C; Cornvik T; Díaz-Moreno I; Ubbink M The Transient Complex of Poplar Plastocyanin with Cytochrome *f*: Effects of Ionic Strength and pH. *Biochim. Biophys. Acta, Bioenerg* 2005, 1707, 179–188.
 - (20). Albarran C; Navarro JA; De la Rosa MA; Hervas M The Specificity in the Interaction between Cytochrome *f* and Plastocyanin from the Cyanobacterium *Nostoc* sp. PCC 7119 Is Mainly Determined by the Copper Protein. *Biochemistry* 2007, 46, 997–1003. [PubMed: 17240983]
 - (21). Scanu S; Foerster JM; Timmer M; Ullmann GM; Ubbink M Loss of Electrostatic Interactions Causes Increase of Dynamics within the Plastocyanin-Cytochrome *f* Complex. *Biochemistry* 2013, 52, 6615–6626. [PubMed: 23984801]
 - (22). Gray JC Cytochrome *f*: Structure, Function and Biosynthesis. *Photosynth. Res* 1992, 34, 359–374. [PubMed: 24408832]
 - (23). Diaz-Moreno I; Diaz-Quintana A; De la Rosa MA; Ubbink M Structure of the Complex between Plastocyanin and Cytochrome *f* from the Cyanobacterium *Nostoc* sp. PCC 7119 as Determined by Paramagnetic NMR. The Balance between Electrostatic and Hydrophobic Interactions within the Transient Complex Determines the Relative Orientation of the Two Proteins. *J. Biol. Chem* 2005, 280, 18908–18915. [PubMed: 15705583]
 - (24). Scanu S; Foerster JM; Ullmann GM; Ubbink M Role of Hydrophobic Interactions in the Encounter Complex Formation of the Plastocyanin and Cytochrome *f* Complex Revealed by Paramagnetic NMR Spectroscopy. *J. Am. Chem. Soc* 2013, 135, 7681–7692. [PubMed: 23627316]
 - (25). Diaz-Moreno I; Diaz-Quintana A; De la Rosa MA; Crowley PB; Ubbink M Different Modes of Interaction in Cyanobacterial Complexes of Plastocyanin and Cytochrome *f*. *Biochemistry* 2005, 44, 3176–3183. [PubMed: 15736928]
 - (26). Schilder J; Ubbink M Formation of Transient Protein Complexes. *Curr. Opin. Struct. Biol* 2013, 23, 911–918. [PubMed: 23932200]

- (27). Hulsker R; Baranova MV; Bullerjahn GS; Ubbink M Dynamics in the Transient Complex of Plastocyanin-Cytochrome *f* from *Prochlorothrix hollandica*. *J. Am. Chem. Soc* 2008, 130, 1985–1991. [PubMed: 18201089]
- (28). Chin JK; Jimenez R; Romesberg FE Direct Observation of Protein Vibrations by Selective Incorporation of Spectroscopically Observable Carbon-Deuterium Bonds in Cytochrome *c*. *J. Am. Chem. Soc* 2001, 123, 2426–2427. [PubMed: 11456893]
- (29). Suydam IT; Boxer SG Vibrational Stark Effects Calibrate the Sensitivity of Vibrational Probes for Electric Fields in Proteins. *Biochemistry* 2003, 42, 12050–12055. [PubMed: 14556636]
- (30). Adhikary R; Zimmermann J; Romesberg FE Transparent Window Vibrational Probes for the Characterization of Proteins with High Structural and Temporal Resolution. *Chem. Rev* 2017, 117, 1927–1969. [PubMed: 28106985]
- (31). Hamm P; Zanni M Concepts and Methods of 2D Infrared Spectroscopy; Cambridge University Press: New York, 2011; p 286.
- (32). Le Sueur AL; Schaugaard RN; Baik MH; Thielges MC Methionine Ligand Interaction in a Blue Copper Protein Characterized by Site-Selective Infrared Spectroscopy. *J. Am. Chem. Soc* 2016, 138, 7187–7193. [PubMed: 27164303]
- (33). Chung JK; Thielges MC; Fayer MD Dynamics of the Folded and Unfolded Villin Headpiece (HP35) Measured with Ultrafast 2D IR Vibrational Echo Spectroscopy. *Proc. Natl. Acad. Sci. U. S. A* 2011, 108, 3578–3583. [PubMed: 21321226]
- (34). Ramos S; Horness RE; Collins JA; Haak D; Thielges MC Site-Specific 2D IR Spectroscopy: A General Approach for the Characterization of Protein Dynamics with High Spatial and Temporal Resolution. *Phys. Chem. Chem. Phys* 2019, 21, 780–781. [PubMed: 30548035]
- (35). Bloem R; Koziol K; Waldauer SA; Buchli B; Walser R; Samatanga B; Jelesarov I; Hamm P Ligand Binding Studied by 2D IR Spectroscopy Using the Azidohomoalanine Label. *J. Phys. Chem. B* 2012, 116, 13705–13712. [PubMed: 23116486]
- (36). King JT; Kubarych KJ Site-specific coupling of hydration water and protein flexibility studied in solution with ultrafast 2D-IR spectroscopy. *J. Am. Chem. Soc* 2012, 134, 18705–18712. [PubMed: 23101613]
- (37). King JT; Arthur EJ; Brooks CL, III; Kubarych KJ Crowding Induced Collective Hydration of Biological Macromolecules Over Extended Distances. *J. Am. Chem. Soc* 2014, 136, 188–194. [PubMed: 24341684]
- (38). Bandaria JN; Dutta S; Nydegger MW; Rock W; Kohen A; Cheatum CM Characterizing the Dynamics of Functionally Relevant Complexes of Formate Dehydrogenase. *Proc. Natl. Acad. Sci. U. S. A* 2010, 107, 17974–17979. [PubMed: 20876138]
- (39). Dutta S; Li Y-L; Rock W; Houtman JCD; Kohen A; Cheatum CM 3-Picolyl Azide Adenine Dinucleotide as a Probe of Femtosecond to Picosecond Enzyme Dynamics. *J. Phys. Chem. B* 2012, 116, 542–548. [PubMed: 22126535]
- (40). Le Sueur AL; Schaugaard RN; Baik M-H; Thielges MC Methionine Ligand Interaction in a Blue Copper Protein Characterized by Site-Selective Infrared Spectroscopy. *J. Am. Chem. Soc* 2016, 138, 7187–7193. [PubMed: 27164303]
- (41). Martinez SE; Huang D; Szczepaniak A; Cramer WA; Smith JL Crystal Structure of Chloroplast Cytochrome *f* Reveals a Novel Cytochrome Fold and Unexpected Heme Ligation. *Structure* 1994, 2, 95–105. [PubMed: 8081747]
- (42). Schultz KC; Supekova L; Ryu Y; Xie J; Perera R; Schultz PG A Genetically Encoded Infrared Probe. *J. Am. Chem. Soc* 2006, 128, 13984–13985. [PubMed: 17061854]
- (43). Park S; Kwak K; Fayer MD Ultrafast 2D-IR Vibrational Echo Spectroscopy: A Probe of Molecular Dynamics. *Laser Phys. Lett* 2007, 4, 704–718.
- (44). Basom EJ; Spearman JW; Thielges MC Conformational Landscape and the Selectivity of Cytochrome P450cam. *J. Phys. Chem. B* 2015, 119, 6620–6627. [PubMed: 25955684]
- (45). Ramos S; Scott KJ; Horness RE; Le Sueur AL; Thielges MC Extended Timescale 2D IR Probes of Proteins: *p*-cyanoselenophenylalanine. *Phys. Chem. Chem. Phys* 2017, 19, 10081–10086. [PubMed: 28367555]

- (46). Kwak K; Park S; Finkelstein IJ; Fayer MD Frequency-Frequency Correlation Functions and Apodization in Two-Dimensional Infrared Vibrational Echo Spectroscopy: A New Approach. *J. Chem. Phys* 2007, 127, 124503. [PubMed: 17902917]
- (47). Kubo R In *Advances in Chemical Physics: Stochastic Processes in Chemical Physics*; Schuler KE; John Wiley & Sons: New York, 1969; Vol. 15, pp 101–127.
- (48). Sykes AG Tilden Lecture. Structure and Electron-Transfer Reactivity of the Blue Copper Protein Plastocyanin. *Chem. Soc. Rev* 1985, 14, 283–315.
- (49). Horness RE; Basom EJ; Thielges MC Site-Selective Characterization of Src Homology 3 Domain Molecular Recognition with Cyanophenylalanine Infrared Probes. *Anal. Methods* 2015, 7, 7234–7241. [PubMed: 26491469]
- (50). Basom EJ; Maj M; Cho M; Thielges MC Site-Specific Characterization of Cytochrome P450cam Conformations by Infrared Spectroscopy. *Anal. Chem* 2016, 88, 6598–6606. [PubMed: 27185328]
- (51). Boxer SG Stark Realities. *J. Phys. Chem. B* 2009, 113, 2972–2983. [PubMed: 19708160]
- (52). Fafarman AT; Sigala PA; Herschlag D; Boxer SG Decomposition of Vibrational Shifts of Nitriles into Electrostatic and Hydrogen-Bonding Effects. *J. Am. Chem. Soc* 2010, 132, 12811–12813. [PubMed: 20806897]
- (53). Kim H; Cho M Infrared Probes for Studying the Structure and Dynamics of Biomolecules. *Chem. Rev* 2013, 113, 5817–5847. [PubMed: 23679868]
- (54). Blasiak B; Ritchie AW; Webb LJ; Cho M Vibrational Solvatochromism of Nitrile Infrared Probes: Beyond the Vibrational Stark Dipole Approach. *Phys. Chem. Chem. Phys* 2016, 18, 18094–18111. [PubMed: 27326899]
- (55). Fayer MD Dynamics of Water Interacting with Interfaces, Molecules, and Ions. *Acc. Chem. Res* 2012, 45, 3–14. [PubMed: 21417263]
- (56). Laage D; Stirnemann G; Sterpone F; Rey R; Hynes JT Reorientation and Allied Dynamics in Water and Aqueous Solutions. *Annu. Rev. Phys. Chem* 2011, 62, 395–416. [PubMed: 21219140]
- (57). Worrall JAR; Liu Y; Crowley PB; Nocek JM; Hoffman BM; Ubbink M Myoglobin and Cytochrome b5: A Nuclear Magnetic Resonance Study of a Highly Dynamic Protein Complex. *Biochemistry* 2002, 41, 11721–11730. [PubMed: 12269814]
- (58). Xu X; Reinle W; Hannemann F; Konarev PV; Svergun DI; Bernhardt R; Ubbink M Dynamics in a Pure Encounter Complex of Two Proteins Studied by Solution Scattering and Paramagnetic NMR Spectroscopy. *J. Am. Chem. Soc* 2008, 130, 6395–6403. [PubMed: 18439013]
- (59). Ramos S; Basom EJ; Thielges MC Conformational Change Induced by Putidaredoxin Binding to Ferrous CO-Ligated Cytochrome P450cam Characterized by 2D IR Spectroscopy. *Front. Mol. Biosci* 2018, 5, 94. [PubMed: 30483514]
- (60). Bashir Q; Volkov A; Ullmann GM; Ubbink M Visualization of the Encounter Ensemble of the Transient Electron Transfer Complex of Cytochrome *c* and Cytochrome *c* Peroxidase. *J. Am. Chem. Soc* 2010, 132, 241–247. [PubMed: 19961227]
- (61). Volkov AN; Bashir Q; Worrall JA; Ullmann GM; Ubbink M Shifting the Equilibrium between the Encounter State and the Specific Form of a Protein Complex by Interfacial Point Mutations. *J. Am. Chem. Soc* 2010, 132, 11487–11495. [PubMed: 20672804]

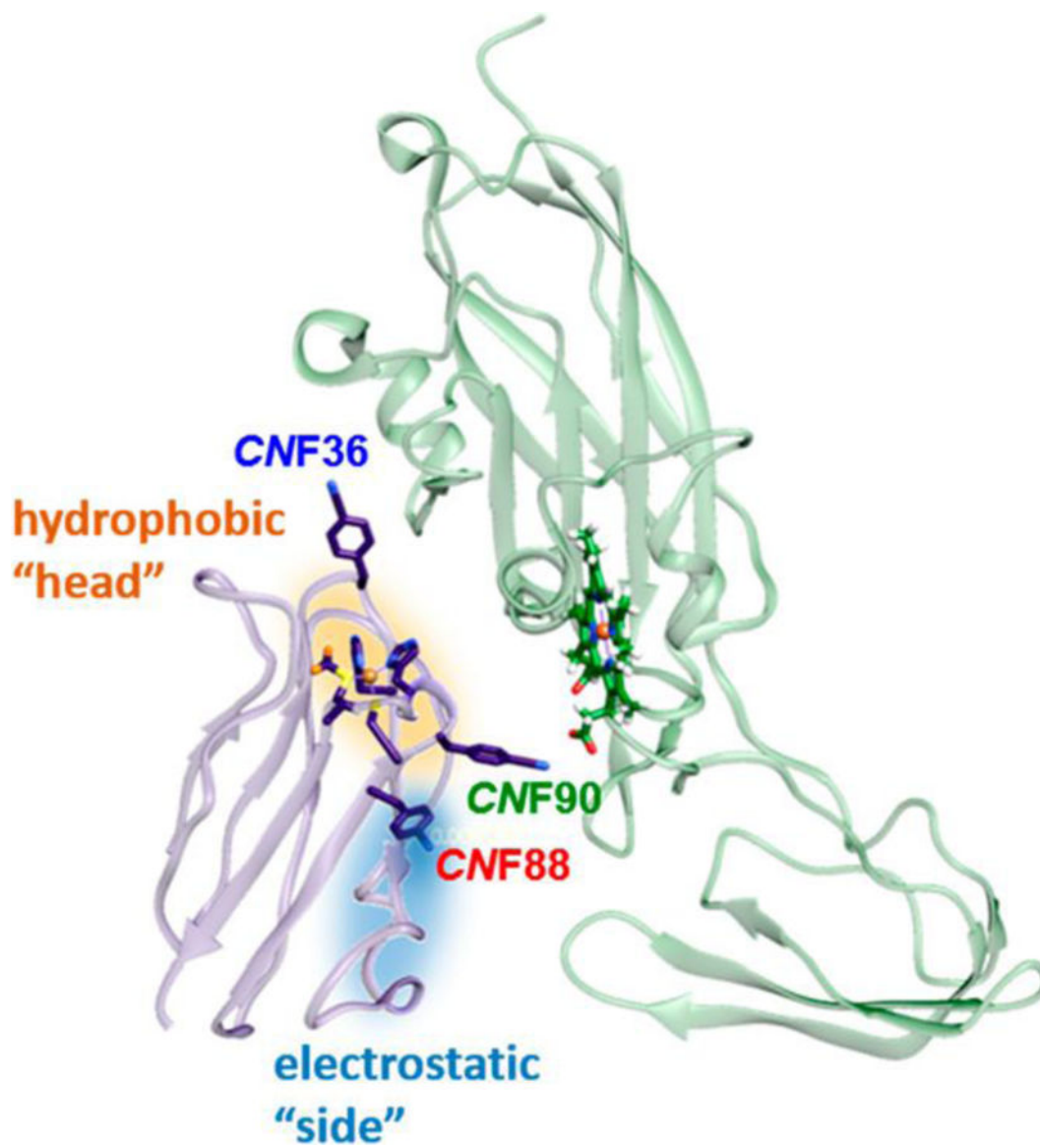


Figure 1. Structural model of the Pc-cyt *f* complex (PDB 1TU2) highlighting introduced CNF probes and the hydrophobic (orange) and electrostatic (blue) patches. Figure was made in UCSF Chimera.⁸

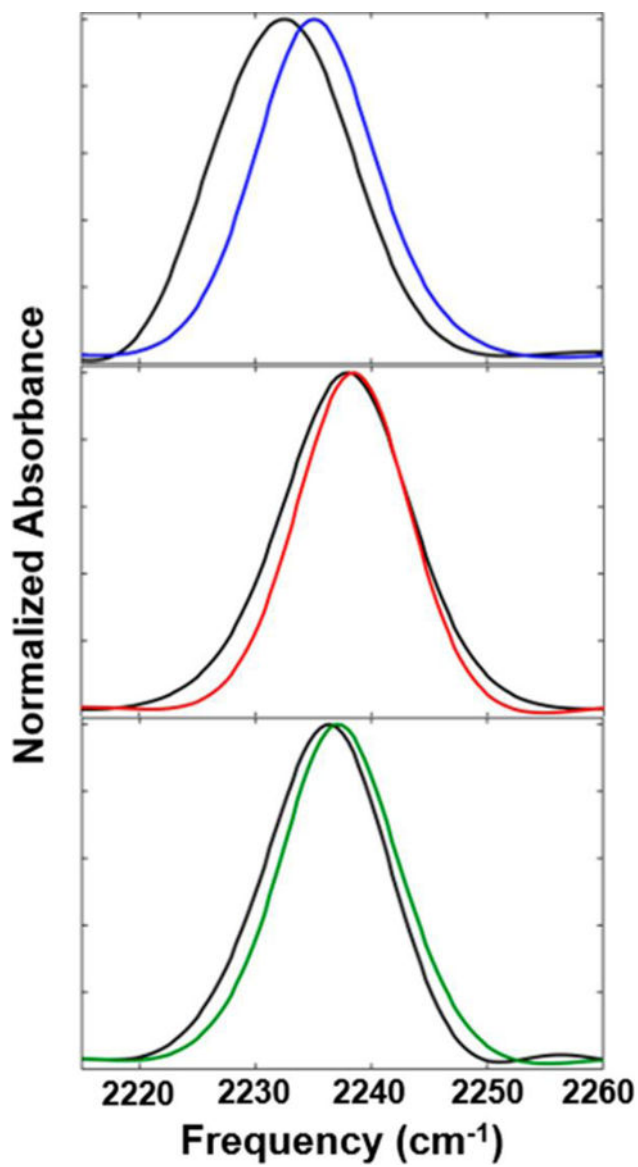


Figure 2. FT-IR spectra of the free Pc (colored lines) and the complex with cyt *f* (black lines) for CMF36 (top), CMF88 (center), and CMF90 (bottom).

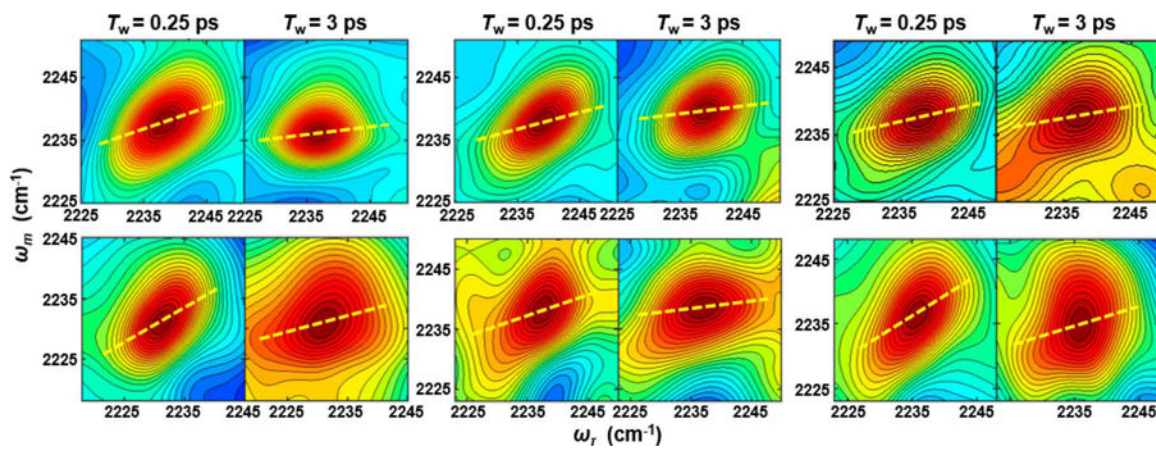


Figure 3.

Representative 2D-IR spectra at T_w of 0.25 and 3 ps for free Pc (top panels) and the complex with cyt *f* (bottom panels) for *CMF36* (left), *CMF88* (center), and *CMF90* (right). The center lines determined from the average spectra are shown as yellow dashed lines.

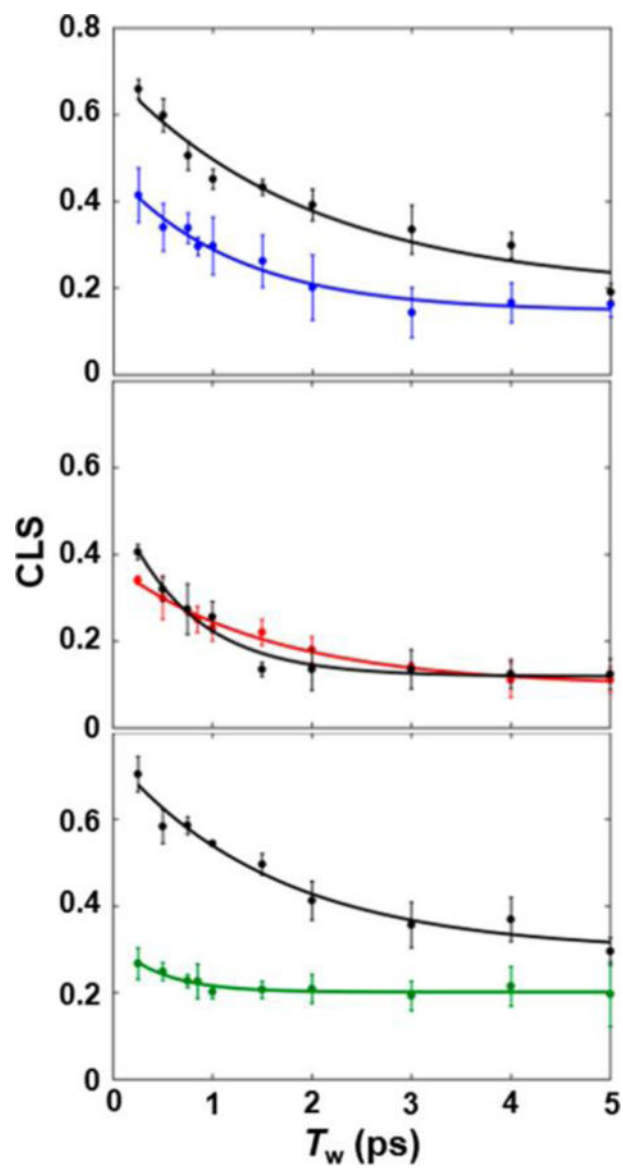


Figure 4. CLS decay curves (points) and fits (lines) for free Pc (colored) and the complex with cyt *f* (black) for *CMF36* (top), *CMF88* (center), and *CMF90* (bottom).

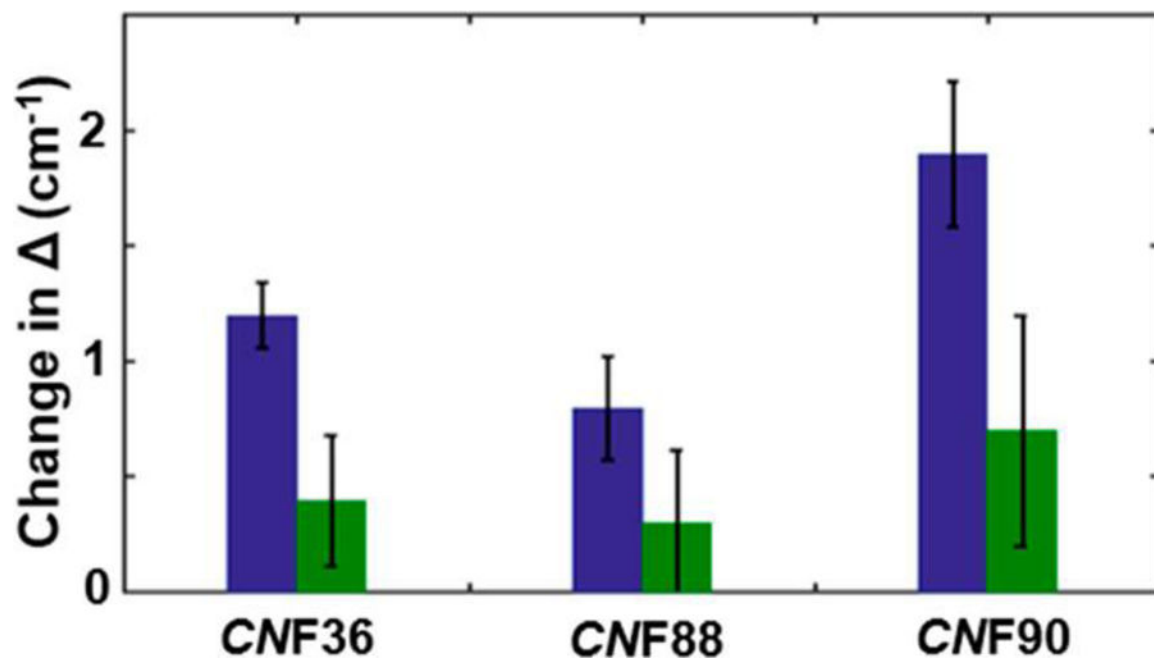


Figure 5. Bar graphs depicting the change in frequency distribution, ν_1 , associated with fast (1 to 2 ps) dynamics (blue) and frequency distribution, ν_5 , associated with slow (>5 ps) dynamics (green) upon binding cyt *f*.

Table 1.

Table of FFCF Parameters and FT-IR Fits

	Γ^* (cm ⁻¹)	Γ (cm ⁻¹)	τ_1 (ps)	s (cm ⁻¹)	frequency (cm ⁻¹) ^a	line width (cm ⁻¹) ^a
CNF	7.9 ± 0.2	2.7 ± 0.2	1.2 ± 0.2	1.5 ± 0.1	2236.7 ± 0.02	12.6 ± 0.1
V36CNF	7.5 ± 0.3	3.0 ± 0.1	1.1 ± 0.2	2.2 ± 0.2	2235.2 ± 0.1	12.6 ± 0.3
V36CNF-eyt <i>f</i>	6.4 ± 0.5	4.2 ± 0.1	2.0 ± 0.3	2.6 ± 0.2	2232.4 ± 0.1	13.5 ± 0.8
Y88CNF	7.2 ± 0.2	2.7 ± 0.2	1.5 ± 0.2	1.6 ± 0.1	2238.4 ± 0.1	11.9 ± 0.2
Y88CNF-eyt <i>f</i>	9.4 ± 0.4	3.5 ± 0.1	0.7 ± 0.1	1.9 ± 0.3	2237.8 ± 0.1	13.2 ± 0.2
E90CNF	9.6 ± 0.6	1.6 ± 0.3	1.2 ± 1.0	2.1 ± 0.4	2237.2 ± 0.1	11.6 ± 0.6
E90CNF-eyt <i>f</i>	5.6 ± 0.4	3.5 ± 0.1	1.6 ± 0.3	2.8 ± 0.3	2236.1 ± 0.2	12.2 ± 0.3

^aFrequency and full width at half-maximum line width from Gaussian fit to 1D spectra.